The Catalytic Decarboxylation of Cyanoacetic Acid: Anionic Tungsten Carboxylates as Homogeneous Catalysts

Donald J. Darensbourg,* Jennifer A. Chojnacki, and Earl V. Atnip

Contribution from the Department of Chemistry, Texas A&M University, College Station, Texas 77843

Received October 22, 1992

Abstract: Cyanoacetic acid was observed to catalytically decompose to its component parts, CO_2 and CH_3CN, in the presence of soluble tungsten(0) carboxylates. In the case in which $W(CO)_5O_2CCH_2CN^-$ was used as the catalyst, the reaction was inhibited by the substrate via an equilibrium process in which the free acid displaced the carboxylate ligand and bound to the metal through the nitrogen atom. The equilibrium constant for this process was measured and determined to be 0.413 at 50 °C, where $k_f = 6.11 \times 10^{-3}$ M^{-1} s^{-1} and $k_r = 1.48 \times 10^{-2}$ M^{-1} s^{-1}. Activation parameters for the decarboxylation process were determined and yielded $\Delta H^* = 21.0 \pm 0.7$ kcal·mol^{-1} and $\Delta S^* = -3.4 \pm 1.9$ eu. The rate limiting step is proposed to be loss of cis CO from the metal with concomitant formation of *cis*-$W(CO)_4(O_2CCH_2CN)(NCCH_2COOH)^-$, since the free energy of activation is quite similar to that for cis carbonyl loss, 23.0 ± 0.9 kcal·mol^{-1}. Subsequent proton transfer and CO_2 loss are fast relative to cis CO displacement. The carboxylate ligand acts as an intramolecular Lewis base, mediating the proton-transfer steps. This was demonstrated by the use of $W(CO)PPh_2(CH_2)_nX^-$ (n = 1 or 2, X = base) as catalysts for the same decarboxylation. Detailed kinetic studies and a proposed mechanism are presented.

Introduction

It has long been known that (cyanomethyl)copper(I) is a reversible CO_2 carrier in the presence of tri-*n*-butylphosphine.[1] However, the discrete molecular complex involved in this process as well as the mechanistic aspects of the reaction are still unknown. Relevant to this reaction (eq 1), we have extensively studied the mechanistic pathway for carbon dioxide insertion into alkyl- and aryltungsten carbonyl derivatives.[2] These investigations demonstrated that the introduction of electron-donating phosphine ligands to the metal center greatly enhanced the rate of CO_2 insertion into the M–R bond. However, unlike the copper(I) systems, the tungsten carboxylates were quite stable toward the reverse reaction, decarboxylation. Furthermore, electron-withdrawing substituents attached to the α-carbon atom of W–alkyl ligands greatly retarded the CO_2 insertion reaction. For example, when X = CN, reaction 2 did not occur even in liquid carbon dioxide.[3]

$$[M]\text{—}R + CO_2 \rightleftharpoons [M]\text{—}O_2CR \qquad (1)$$

$$\underset{\mathbf{1}}{(CO)_5W\text{–}CH_2(X)^-} + CO_2 \rightarrow \underset{\mathbf{2}}{(CO)_5W\text{–}O_2CCH_2(X)^-} \qquad (2)$$

The solid-state structure of **1** displays a W–CH_2CN bond distance of 2.330(8) Å, which is quite similar to that noted for the W–CH_3 bond in $(CO)_5WCH_3^-$ of 2.313(17) Å. This latter derivative readily undergoes carboxylation at modest CO_2 pressures to afford the metal acetate species. Hence, it was concluded that it is the decrease in nucleophilicity of the metal center containing the $-CH_2CN$ group as opposed to a stronger W–C bond that retards the rate of CO_2 reacting with **1** compared with $(CO)_5WCH_3^-$. Nevertheless, complex **2** was easily prepared by the displacement of the labile THF ligand in photogenerated $W(CO)_5THF$ by the $O_2CCH_2CN^-$ anion. Like all $(CO)_5WO_2CR^-$ derivatives, complex **2** readily dissociates cis CO ligands.[4] In this instance, the first-order rate constant for CO loss is 7.44×10^{-4} s^{-1} at 40 °C in THF, with $\Delta H^* = 25.3 \pm 0.8$ kcal·mol^{-1} and $\Delta S^* = 7.7 \pm 2.5$ eu. These kinetic parameters are greatly influenced by the nature of the R substituent, with electron-releasing R groups leading to more labile CO ligands. For example, for R = $C(CH_3)_3$, k_1 has a value of 1.09×10^{-2} s^{-1} at 40 °C.

Although $W(CO)_5O_2CCH_2CN^-$ does not itself undergo decarboxylation, it effectively catalyzes the decarboxylation of cyanoacetic acid. In the presence of protic acids, the cyanoacetate ligand in **2** is protonated and rearranges to the nitrogen-bound cyanoacetic acid derivative, $W(CO)_5NCCH_2COOH$ (**3**).[5] Dependent on the nature and concentration of the added acid, an equilibrium exists in solution between **2** and **3** (eq 3). We report herein a description of the role of complex **2** in the homogeneous catalytic decarboxylation of cyanoacetic acid.

$$\underset{\mathbf{2}}{W(CO)_5O_2CCH_2CN^-} + H^+ \rightleftharpoons \underset{\mathbf{3}}{W(CO)_5NCCH_2COOH} \qquad (3)$$

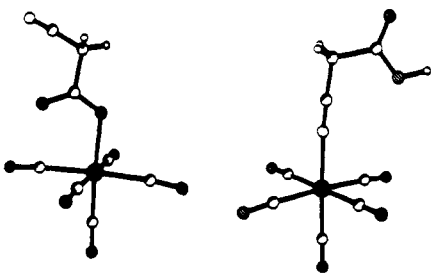

(1) (a) Tsuda, T.; Nakatsuka, T.; Hirayama, T.; Saegusa, T. *J. Chem. Soc., Chem. Commun.* **1974**, 557. (b) Tsuda, T.; Chajo, Y.; Saegusa, T. *J. Am. Chem. Soc.* **1977**, *99*, 1648.

(2) (a) Darensbourg, D. J.; Kudaroski, R.; Bausch, C. G.; Pala, M.; Simmons, D.; White, J. N. *J. Am. Chem. Soc.* **1985**, *107*, 7463. (b) Darensbourg, D. J.; Kudaroski, R. *J. Am. Chem. Soc.* **1984**, *106*, 3672. (c) Darensbourg, D. J.; Wiegreffe, H. P. *Inorg. Chem.* **1990**, *29*, 592. (d) Darensbourg, D. J.; Grötsch, G. *J. Am. Chem. Soc.* **1985**, *107*, 7473.

(3) Darensbourg, D. J.; Joyce, J. A.; Rheingold, A. *Organometallics* **1991**, *10*, 3407.

(4) Darensbourg, D. J.; Joyce, J. A.; Bischoff, C. J.; Reibenspies, J. H. *Inorg. Chem.* **1991**, *30*, 1137.

(5) Darensbourg, D. J.; Atnip, E. V.; Reibenspies, J. H. *Inorg. Chem.* **1992**, *31*, 4475.

0002-7863/93/1515-4675$04.00/0

Experimental Section

Materials. All manipulations were carried out in an argon-filled dry box or on a double manifold vacuum/N_2 line. Solvents were dried by standard methods and distilled under a nitrogen atmosphere prior to use. All reagents were commercially available and were used without further purification unless otherwise noted. Experiments utilizing photolysis were performed with a mercury arc 450-W UV immersion lamp purchased from Ace Glass Co. in a water-cooled Pyrex vessel. Infrared spectra were recorded on either an IBM FTIR/32 or a Mattson 6021 Galaxy/FTIR spectrometer. NMR spectra were taken on a Varian XL-200 superconducting high-resolution spectrometer with an internal deuterium lock in 5-mm tubes. GC/MS data were collected on a Hewlett Packard 5890 Series II gas chromatograph coupled with a Hewlett Packard mass selective detector (30 m, 0.25-mm i.d. capillary column).

Synthesis of [PPN][$W(CO)_5O_2CCH_2CN$] (2). The synthesis of this compound has been previously reported.[4] (IR ν_{CO} (DME) 2061 (w), 1911 (s), 1853 (m) cm^{-1}; ^{13}C NMR (acetone-d_6), 201.1 (s) and 205.5 (s) ppm.)

Synthesis of $W(CO)_5NCCH_2CO_2H$ (3). The synthesis of $W(CO)_5NCCH_2COOH$ was accomplished in >90% yield by the reaction of $W(CO)_5THF$ with 1 equiv of $NCCH_2COOH$ in THF solvent at ambient temperature. The THF was removed from the reaction mixture by vacuum and the remaining light yellow-green solid was washed with hexane three times to afford a light green powder. Anal. Calcd for $W(CO)_5NCCH_2COOH$ ($C_8H_3NO_7W$): C, 23.50; H, 0.74. Found: C, 23.42; H, 0.85. Molecular weight determined by vapor phase osmometry; found, 418 (calcd, 408.96). (IR ν_{CO} (THF) 2075 (w), 1938 (vs), 1908 (m) cm^{-1}; ^{13}C NMR (acetone-d_6) 196.5 (s) and 199.9 (s) ppm.)

Synthesis of [PPN][$W(CO)_4(\eta^2$-$PPh_2CH_2CO_2)$]. This complex was prepared by the reaction of $W(CO)_5THF$ with 1 equiv of Ph_2PCH_2COOH in THF solvent. The resulting $W(CO)_5PPh_2CH_2COOH$ complex (ν_{CO} in THF, 2072 (w) and 1934 (s) cm^{-1}) was isolated as a solid upon removal of the solvent. This phosphine carboxylic acid complex was deprotonated with 1 equiv of NaH in THF with stirring for 45 min. The solvent was removed from the reaction mixture under vacuum, and the remaining light yellow powder was washed three times with hexane. The powder was dissolved in 20 mL of acetonitrile and cannulated into a 50-mL Schlenk flask containing 1 equiv of [PPN][Cl]. This solution was stirred for 15 min and allowed to stand for an additional 15 min at ambient temperature during which time NaCl precipitated from solution. Loss of CO occurred with concomitant chelation of the ligand upon gentle warming of the solution and removal of CO with a nitrogen stream. The resultant solution was filtered through Celite. Acetonitrile was removed from the filtrate by vacuum, and the desired [PPN][$W(CO)_4PPh_2CH_2CO_2$] complex (ν_{CO} (CH_3CN), 2003 (w), 1877 (s), 1811 (m) cm^{-1}) was isolated by filtration and dried.

Synthesis of [PPN][*cis*-$W(CO)_4(NCCH_2COOEt)(O_2CCH_2CN)$]. The synthesis of *cis*-$W(CO)_4(NCCH_2COOEt)(O_2CCH_2CN)^-$ was accomplished by refluxing a THF solution of [PPN][$W(CO)_5(O_2CCH_2CN)$] with a 10% molar excess of $NCCH_2COOEt$ for 24 h. The resulting *cis*-$W(CO)_4(NCCH_2COOEt)(O_2CCH_2CN)^-$anion (IR ν_{CO} (THF) 1993 (w), 1861 (s), 1845 (sh), 1801 (m) cm^{-1}) did not decarboxylate, and all attempts at crystallization of the PPN^+ salt failed.

Attempted Syntheses of $W(CO)_5ICH_2COOH$ and $W(CO)_5ClCH_2COOH$. The syntheses of $W(CO)_5ICH_2COOH$ and $W(CO)_5ClCH_2COOH$ were attempted by the reaction of $W(CO)_5THF$ with 1 equiv of ICH_2COOH or $ClCH_2COOH$, respectively. The reactions did not yield the desired products. After the reaction mixtures were stirred for 6 h at ambient temperature, an infrared spectrum of the mixtures indicated the presence of only $W(CO)_6$, $W(CO)_5THF$, and the free acids, ICH_2COOH or $ClCH_2COOH$.

Synthesis of [PPN][$W(CO)_4(\eta^2$-$PPh_2CH_2CH_2S)$]. The synthesis of [PPN][$W(CO)_4(PPh_2CH_2CH_2S)$] was accomplished by the reaction of [PPN][$W(CO)_5Me$] with 1 equiv of $PPh_2CH_2CH_2SH$ in THF. The mixture was stirred for 24 h followed by removal of the THF under reduced pressure. The resulting [PPN][$W(CO)_4(PPh_2CH_2CH_2S)$] complex (IR ν_{CO} 1991 (w), 1871 (br), 1805 (m) cm^{-1}) was isolated by filtration.

Catalytic Decarboxylation of $NCCH_2COOH$ by 2. The catalytic decarboxylation of cyanoacetic acid to form acetonitrile and carbon dioxide using **2** as a catalyst was observed by infrared spectroscopy in DME solution. In a typical experiment, a solution of **2** (0.114 g, 0.121 mmol, in 10 mL of DME) was added to a flask containing HO_2CCH_2CN (0.160 g, 1.88 mmol) and the resulting yellow solution was heated at 65 °C. The disappearance of the strong ν_{COO} band of the acid at 1747 cm^{-1} was observed with concomitant appearance of the ν_{CN} band of acetonitrile at 2253 cm^{-1} and the ν_{COO} band of CO_2 at 2338 cm^{-1}. The decarboxylation was also evidenced by GC/MS data. A solution of HO_2CCH_2CN (0.104 g, 1.22 mmol in 10 mL of THF) was added to a flask containing **2** (0.115 g, 0.122 mmol). The solution was heated at 68 °C and monitored by infrared spectroscopy until all of the acid had been consumed (approximately 2.5 h). Acetonitrile (m/z = 41), carbon dioxide (m/z = 44), and several fragments of the metal complex were detected. There was no evidence of succinonitrile (m/z = 80) in the solution.

The kinetics of the catalytic decomposition of HO_2CCH_2CN were monitored by infrared spectroscopy. Solution temperatures were controlled by a thermostated water bath with a precision of ±0.1 °C. A prepared solution of HO_2CCH_2CN (10 mL of 0.194 M acid in DME) was equilibrated to the desired temperature and transferred via cannula to a flask containing solid **2** (0.115 g, 0.122 mmol). Small aliquots of solution (≈0.2 mL) were withdrawn periodically by syringe and examined by IR. The rate of catalysis was monitored by following the disappearance of the ν_{COO} band of the acid at 1747 cm^{-1}. A base-line correction was made on each spectrum by subtracting the absorbance in a region free of any peaks. This value was arbitrarily chosen as 2200 cm^{-1}. Rate constants were determined from the slope of a plot of ln A_t vs time where A_t is [(intensity at 1747 cm^{-1}) − (intensity at 2200 cm^{-1})] at a time, t; this gave a nearly linear plot for the bulk of the reaction time (see Figure 4). The first-order rate constants were divided by the equilibrium concentration of **2** in the reaction mixture, as determined from a Beer's law analysis, to remove the dependence on [**2**]. Activation parameters were determined by the method of Christian and Tucker.[6]

Photochemical Decarboxylation of $NCCH_2COOH$ Catalyzed by 2. A sample of **2** was photolyzed in THF while bubbling nitrogen through the solution to produce [PPN][$W(CO)_4(O_2CCH_2CN)(THF)$]. The solution was then transferred from the photolysis cell to a 50-mL flask immersed in a −78 °C bath. To this solution was added 1 equiv of $NCCH_2COOH$. An infrared spectrum collected immediately after the addition of the $NCCH_2COOH$ at room temperature indicated production of 1 equiv of CO_2 and regeneration of $W(CO)_5(O_2CCH_2CN)^-$ and a trace of $W(CO)_6$.

Rate of Catalytic Decarboxylation of $NCCH_2COOH$ by 2 with Added CH_3CN. The kinetics of the catalytic decarboxylation of HO_2CCH_2CN in the presence of added acetonitrile were monitored by infrared spectroscopy. A solution of **2** (0.115 g, 0.122 mmol, in 9.9 mL of DME) was equilibrated to 65 °C in a thermostated water bath. The solution was transferred to a flask containing HO_2CCH_2CN (0.162 g, 1.90 mmol) and CH_3CN (0.10 mL, 1.91 mmol). The rate of decarboxylation of HO_2CCH_2CN was monitored by infrared spectroscopy as described above.

Rate of Catalytic Decarboxylation of $NCCH_2COOH$ by 2 under CO. The rate of catalytic decarboxylation of HO_2CCH_2CN by **2** under a pressure of carbon monoxide gas was monitored by infrared spectroscopy. A solution of HO_2CCH_2CN (0.174 g, 2.046 mmol, in 10 mL of DME) was added to a flask containing **2** (0.250 g, 0.264 mmol), and the resulting solution was immediately transferred to a high-pressure reactor fitted with a ZnSe crystal rod. The reactor was heated to 65 °C and pressurized to 500 psi with CO gas, and the solution was stirred. Spectra were taken in situ throughout the course of the reaction. The rate of the reaction was monitored by following the disappearance of the acid band at 1747 cm^{-1} as a function of time. A base-line correction was made on each spectrum. The observed rate constant was determined from a linear plot of ln Abs_{1747} vs time. For comparison, the identical experiment was done using 500 psi of N_2 gas in place of the CO gas. The pseudo-first-order rate constant was found to be 3.11×10^{-4} s^{-1} under 500 psi of CO and 1.45×10^{-4} s^{-1} under N_2.

Catalytic Decarboxylation of $NCCH_2COOH$ by [PPN][$W(CO)_4(PPh_2CH_2COO)$]. A 20-mL DME solution containing 0.671 g (0.623 mmol) of [PPN][$W(CO)_4(PPh_2CH_2COO)$] was placed in a 65 °C constant temperature bath. To this solution was added a 5-mL DME solution containing 0.794 g (9.33 mmol) of $NCCH_2COOH$. Rate data were collected by following the disappearance of the ν_{COO} infrared band of the free $NCCH_2COOH$. A pseudo-first-order plot of these data is provided in the supplementary material.

Catalytic Decarboxylation of $NCCH_2COOH$ by $W(CO)_4(PPh_2CH_2CH_2NMe_2)$. The $W(CO)_4(PPh_2CH_2CH_2NMe_2)$ complex was supplied by Professor G. R. Dobson.[7] A 20-mL DME solution containing 0.250 g (0.452 mmol) of $W(CO)_4(PPh_2CH_2CH_2NMe_2)$ was placed in

(6) (a) Christian, S. D.; Tucker, E. E. *Am. Lab.* (*Fairfield, Conn.*) **1982**, *14*(8), 36. (b) Christian, S. D.; Tucker, E. E. *Am. Lab.* (*Fairfield, Conn.*) **1982**, *14*(9), 31.

(7) Dobson, G. R.; Dobson, C. B.; Mansour, S. E. *Inorg. Chim. Acta* **1985**, *100*, L7.

a 65 °C constant temperature bath. To this solution was added a 5-mL DME solution containing 0.577 g (6.78 mmol) of $NCCH_2COOH$. Upon addition of the acid, the intermediate, $W(CO)_4(PPh_2CH_2CH_2NMe_2)(NCCH_2COOH)$, was observed by infrared spectroscopy (ν_{CO} 2015 (w), 1904 (sh), 1890 (s), 1860 (m) cm^{-1}). Rate data were collected by following the disappearance of the ν_{COO} infrared band of the free $NCCH_2COOH$.

Catalytic Decarboxylation of $NCCH_2COOH$ by [PPN][$W(CO)_4(PPh_2CH_2CH_2S)$]. A 20-mL DME solution containing 0.221 g (0.205 mmol) of [PPN][$W(CO)_4(PPh_2CH_2CH_2S)$] was placed in a 65 °C constant temperature bath. To this solution was added a 5-mL DME solution containing 0.261 g (3.07 mmol) of $NCCH_2COOH$. Rate data were collected by following the disappearance of the ν_{COO} infrared band of the free $NCCH_2COOH$. A pseudo-first-order plot of these data is provided in the supplementary material.

Catalytic Decarboxylation of $NCCH_2COOH$ by [PPN][$W(CO)_4(PPh_2CH_2CH_2S)$] under 600 psi of CO. [PPN][$W(CO)_4(PPh_2CH_2CH_2S)$] (0.262 g, 0.243 mmol) was placed in a 50-mL Schlenk flask fitted with a rubber septum in a glovebox. The flask was removed from the glovebox and the solid dissolved in 10 mL of DME. A high-pressure reactor fitted with a silicon crystal rod was evacuated and backfilled with argon three times. The cell was again evacuated, and the DME solution of [PPN][$W(CO)_4(PPh_2CH_2CH_2S)$] was transferred via cannula to the cell. The cell was placed directly in the infrared spectrometer sample compartment. The temperature was ramped to 65 °C, and the cell was pressurized with 600 psi of CO. The reaction was monitored by following the disappearance of the ν_{COO} infrared band of the free $NCCH_2COOH$. Over a 3-h reaction period *no* decarboxylation of cyanoacetic acid was observed.

Equilibrium Constant Measurement. The equilibrium constant for the reaction of **2** + $NCCH_2COOH$ to form **3** + $^-O_2CCH_2CN$ was measured by infrared spectroscopy at 50.0 °C and 68.0 °C. A solution of **2** (0.115 g, 0.122 mmol, in 10 mL of DME) that had been equilibrated to 50.0 °C was added to a flask containing an excess of $NCCH_2COOH$ (0.103 g, 1.21 mmol). The reaction was monitored by infrared spectroscopy until equilibrium was reached, approximately 90 min. The equilibrium concentration of **3** was determined from the absorbance of the strong ν_{CO} band (the *E* band) by means of a Beer's law analysis. K_{eq} at 50.0 °C was then determined from

$$K_{eq} = \frac{[\mathbf{3}][^-O_2CCH_2CN]}{[\mathbf{2}][HO_2CCH_2CN]}$$

where $[^-O_2CCH_2CN] = [\mathbf{3}]$, $[\mathbf{2}]_{eq} = \{[\mathbf{2}]_{initial} - [\mathbf{3}]\}$, $[HO_2CCH_2CN]_{eq} = \{[HO_2CCH_2CN]_{initial} - [\mathbf{3}]\}$.

Likewise, the equilibrium constant K_{eq} was determined at 68.0 °C. A 10-mL solution of $NCCH_2COOH$ (0.194 M in DME) was equilibrated to 68.0 °C and added to a flask containing **2** (0.115 g, 1.22 mmol). The reaction was monitored by infrared spectroscopy until equilibrium was reached (approximately 10 min) and throughout the course of the decarboxylation. The equilibrium concentration of **2** was determined from the absorbance of the medium ν_{CO} band by means of a Beer's law analysis. K_{eq} was determined using the above equation where $\{[\mathbf{2}]_{initial} - [\mathbf{2}]_{eq}\} = X$, $[HO_2CCH_2CN] = \{[HO_2CCH_2CN]_{initial} - X\}$, $[\mathbf{3}] = X$, and $[^-O_2CCH_2CN] = X$.

Determination of Equilibrium Rate Constants. Using the data obtained as described above in the determination of K_{eq}, the forward and reverse rate constants were determined at 50.0 °C and 68.0 °C. In the case of

$$\mathbf{2} + NCCH_2COOH \rightleftharpoons \mathbf{3} + {}^-O_2CCH_2CN$$

the following relationship exists:[8]

$$\ln\frac{\Delta}{\alpha + \Delta(1 - K_{eq}^{-1})} = (-k_f)\alpha t + \text{constant}$$

where $\alpha = \{[\mathbf{2}]_\infty + [HO_2CCH_2CN]_\infty + (1/K_{eq})([\mathbf{3}]_\infty + [^-O_2CCH_2CN]_\infty)\}$ and Δ is defined by $\Delta = ([\mathbf{2}]_t - [\mathbf{2}]_\infty)$, $([NCCH_2COOH]_t - [NCCH_2COOH]_\infty)$, $([\mathbf{3}]_\infty - [\mathbf{3}]_t)$, or $([^-O_2CCH_2CN]_\infty - [^-O_2CCH_2CN]_t)$. At 50.0 °C, Δ was defined by $\Delta = \{[\mathbf{3}]_\infty - [\mathbf{3}]_t\}$; the concentrations of **3** were determined from the absorbance of the strong ν_{CO} band (the *E* band) by means of a Beer's law analysis. At 68.0 °C, Δ was defined by $\Delta = \{[\mathbf{2}]_t - [\mathbf{2}]_\infty\}$; the concentrations of **2** were determined from the absorbance of the medium ν_{CO} band by means of a Beer's law analysis. For each temperature, k_f was determined from a plot of $\ln\{\Delta/[\alpha + \Delta(1 - K_{eq}^{-1})]\}$ vs time. The reverse rate k_r was then calculated from $K_{eq} = k_f/k_r$.

(8) King, E. L. *Int. J. Chem. Kinet.* **1982**, *14*, 1285.

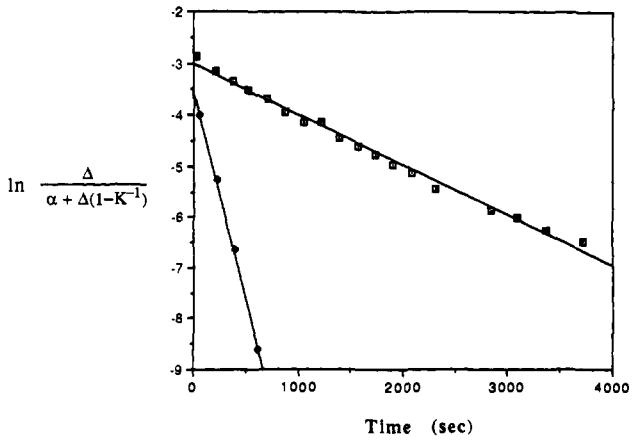

Figure 1. Data plot for the determination of k_f and k_r where the slope equals $(-k_f)\alpha$ at 68 °C (◆) and 50 °C (□).

Molecular Modeling of $W(CO)_4(NCCH_2COOH)(O_2CCH_2CN)^-$. The $W(CO)_4(NCCH_2COOH)(O_2CCH_2CN)^-$ model was assembled from fragments of the previously reported structures of [Et_4N][$W(CO)_5O_2CCH_2CN$][3] and $W(CO)_5NCCH_2COOH$[5]. The $W(CO)_5O_2CCH_2CN^-$ structure file was opened in Chem-X (Chem-X 1989), and one cis carbonyl was deleted. The remaining $W(CO)_4O_2CCH_2CN^-$ fragment was saved. The $W(CO)_5NCCH_2COOH$ structure file was opened, and the $NCCH_2COOH$ fragment was saved. The two fragments were then merged, and a bond was made between W1 and N2. The W1–N2 bond length and N2–W1–C4 and N2–W1–C3 bond angles were set to those found in the $W(CO)_5NCCH_2COOH$ structure. The bonds W1–N2, C9–C10, C10–O7, W1–O5, and O5–C5 were selected for bond rotations, and the N1–H1 distance was displayed. Each of the five bonds was rotated one at a time so as to minimize the N1–H1 distance. This process was repeated until the closest distance between N1 and H1 was achieved.

Reaction of 2 with HO_2CCH_2Cl. A solution of **2** (0.335 g, 0.354 mmol, in 10 mL of DME) was equilibrated to 65 °C and added to a flask containing HO_2CCH_2Cl (0.513 g, 5.43 mmol). Small aliquots were withdrawn by syringe and examined by infrared spectroscopy. After 0.5 h, a small amount of CO_2 gas was seen in solution (2338 cm^{-1}). A shoulder at 1937 cm^{-1} that disappeared with concomitant formation of $W(CO)_6$ (1976 cm^{-1}) was also observed. After 1.5 h, nearly all of the metal complex had decomposed to $W(CO)_6$; the intensity of the ν_{COO} infrared band of $ClCH_2COOH$ at 1756 cm^{-1} did not change.

Reactivity of 2 with H^+ To Form 3. To a solution of **2** (0.116 g, 0.123 mmol, in 10 mL of DME) was added HBF_4 (20 μL, 0.136 mmol) via syringe. The mixture was stirred at room temperature for 10 min and examined by infrared spectroscopy. Likewise, the reaction was carried out under 1 atm of CO gas. The formation of **3** was evidenced by the shift of the three ν_{CO} infrared bands to higher energy. Additionally, the formation of a small amount of $W(CO)_6$ was observed during the reactions by the appearance of a band at 1976 cm^{-1}.

Results

An equilibrium mixture of $W(CO)_5O_2CCH_2CN^-$ (**2**) and its protonated analog, $W(CO)_5NCCH_2COOH$ (**3**), resulted upon addition of cyanoacetic acid to complex **2** in DME solution. The equilibrium constant for reaction 4 was spectroscopically determined at 50.0 °C and 68.0 °C and found to be 0.413 and 0.119, respectively. By way of contrast, upon addition of the strong

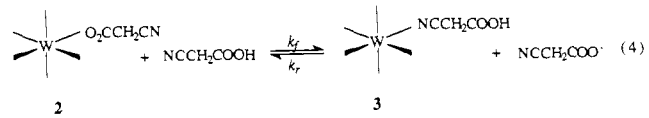

acid HBF_4 to complex **2**, quantitative formation of **3** occurred. The second-order rate constants for the forward and reverse reactions were measured by the method of King[8] and were found to be 6.11×10^{-3} M^{-1} s^{-1} and 1.48×10^{-2} M^{-1} s^{-1} at 50.0 °C and 2.29×10^{-2} M^{-1} s^{-1} and 1.93×10^{-1} M^{-1} s^{-1} at 68.0 °C, respectively. As is seen in Figure 1, the former values are more accurately determined where the approach to equilibrium is slower. It is

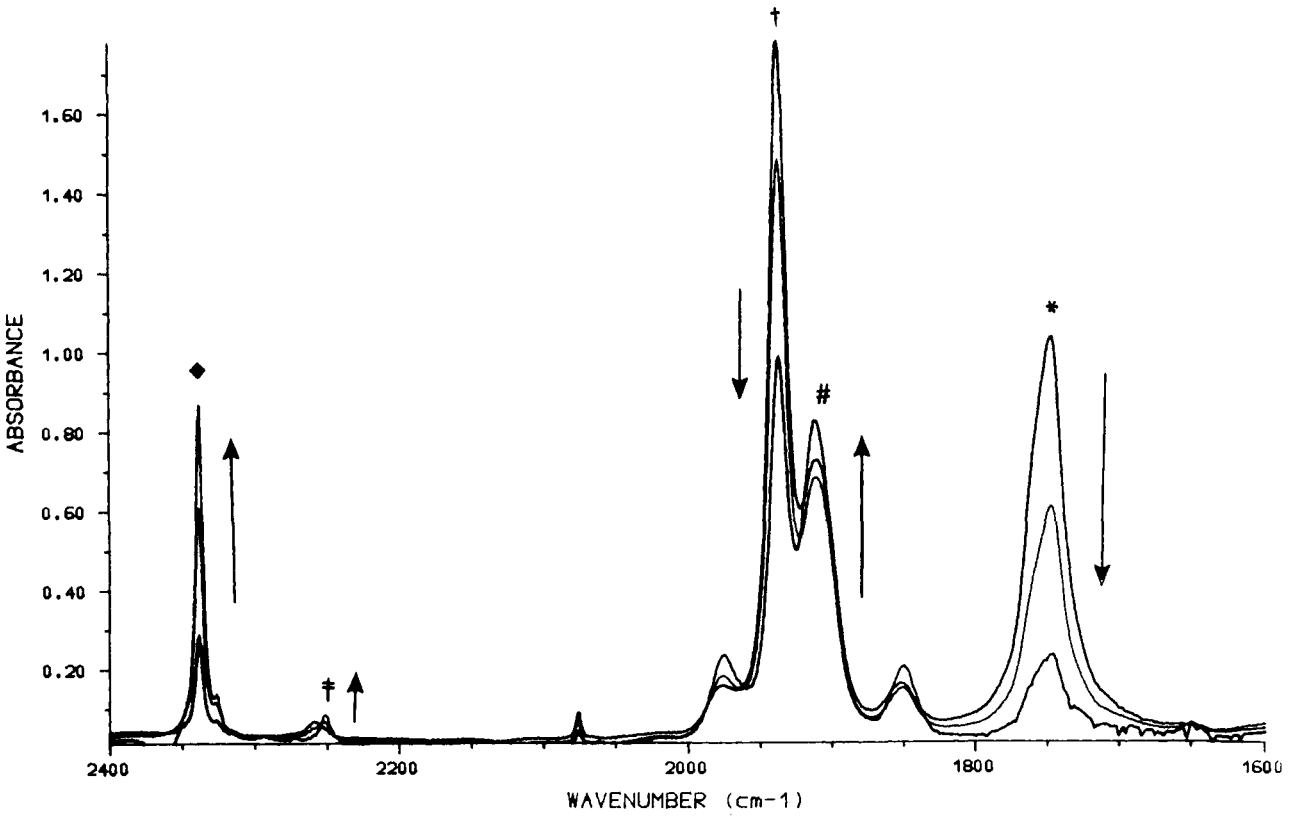

Figure 2. Infrared spectra following the decarboxylation of cyanoacetic acid catalyzed by **2** after the equilibrium between **2** and **3** was established. As the amount of free cyanoacetic acid in solution decreases, the equilibrium shifts to increase the concentration of **2** at the expense of **3**: (*) = $NCCH_2COOH$, (#) = $W(CO)_5O_2CCH_2CN^-$, (†) = $W(CO)_5NCCH_2COOH$, (‡) = CH_3CN, (◆) = CO_2.

important to note that complexes **2** and **3** have been fully characterized, both in solution and in the solid state.

Complex **2** was found to be an effective catalyst or catalyst precursor for the decarboxylation of cyanoacetic acid (eq 5) under mild conditions; in the absence of a catalyst, cyanoacetic acid is known to decompose to CO_2 and CH_3CN at 160 °C. The catalytic

$$NCCH_2COOH \xrightarrow{2} CH_3CN + CO_2 \qquad (5)$$

reactions were monitored by infrared spectroscopy as indicated in Figure 2, where all the reactants and products are evident, i.e., the two metal carbonyl derivatives, the acid substrate, and the CO_2/CH_3CN. The hydrocarbon product was further identified and quantified by GC/MS. There was no succinonitrile ($NCCH_2CH_2CN$) produced in the reaction, indicative of the absence of $NCCH_2$ radicals. As noted in Figure 3, the rate of decarboxylation is inhibited by an increase in the initial concentration of the acid substrate, $NCCH_2COOH$. This is further illustrated in Figure 4, where the rate of catalysis increases as the reaction proceeds with concomitant consumption of the acid and production of **2** at the expense of **3**, that is, the equilibrium in eq 4 shifts to produce the active form of the catalyst, $W(CO)_5O_2CCH_2CN^-$, as the substrate is consumed. At the end of the reaction when all of the cyanoacetic acid was expended, $W(CO)_5O_2CCH_2CN^-$ was the only metal-containing species present and its concentration was the same as its initial concentration. Because of this inhibitory nature of the substrate, $NCCH_2COOH$, a more efficient catalytic process is achieved by pulsing in the substrate in intervals of 16–20 equiv.

It is noteworthy from Figure 5b that the equilibrium in eq 4 is established rapidly with a relatively constant concentration of complex **2** being present during the exponential (initial) portion of the plot of [acid] vs time (Figure 5a). With time (beyond 50 min at 68 °C), the concentration of **2** increases and the rate of acid consumption increases, i.e., there is a positive deviation from the exponential decay of the acid. Although k_f is smaller than k_r for reaction 4, the concentration of $NCCH_2COOH$ greatly exceeds the concentration of its conjugate base, $NCCH_2CO_2^-$, accounting for the fast formation of **3** from **2** and the rather slow return of complex **2** from **3**. Hence, it is possible to conclude from the data in Figures 3 and 5 that catalytic activity is intimately associated with the concentration of complex **2**.

This dependency on the concentration of complex **2** is further demonstrated in Figure 3, where the estimated value of k_{obsd} at $[acid]_0 = 0$ was determined to be $8.3 \pm 3.0 \times 10^{-4}$ s^{-1}. This represents the uninhibited or fastest rate of decarboxylation of cyanoacetic acid catalyzed by complex **2** under these reaction conditions. This value of k_{obsd} is consistent with the value calculated from the rate data. As shown in Figure 5, $[2]_{eq} = 3.27 \times 10^{-3}$ M and $[2]_0 = 1.22 \times 10^{-2}$ M with a $k_{obs} = 1.61 \times 10^{-4}$ s^{-1}. This data gives a value of $[2]_0/[2]_{eq} = 3.72$. Thus, the maximum rate constant (i.e., at [acid] = 0) is $3.72k_{obsd}$, or $k_{obsd} = 5.98 \times 10^{-4}$ s^{-1}. This calculated value of k_{obsd} is within the error limits of the measured k_{obsd} at $[acid]_0 = 0$ of $(8.3 \pm 3.0) \times 10^{-4}$ s^{-1}.

The kinetic parameters for the decarboxylation of cyanoacetic acid catalyzed by **2** were determined as a function of temperature over a range of 16 °C in DME. These data are listed in Table I. Since the reaction is first order in both catalyst concentration and acid concentration, it was necessary to correct these constants for the concentration of species **2**. This represents the equilibrium concentration of **2** obtained for a given initial concentration of acid from data as illustrated in Figure 5b in the boxed area. These second-order rate contants (k_2) are shown as well in Table I. The corresponding activation parameters obtained were $\Delta H^* = 21.0 \pm 0.7$ kcal·mol^{-1} and $\Delta S^* = -3.4 \pm 1.9$ eu. An Eyring plot of the data contained in Table I is depicted in Figure 6.

The decarboxylation reaction (eq 5) using **2** as a catalyst was performed under a pressure of carbon monoxide (500 psi) at 65 °C and monitored in situ by infrared spectroscopy. The rate of

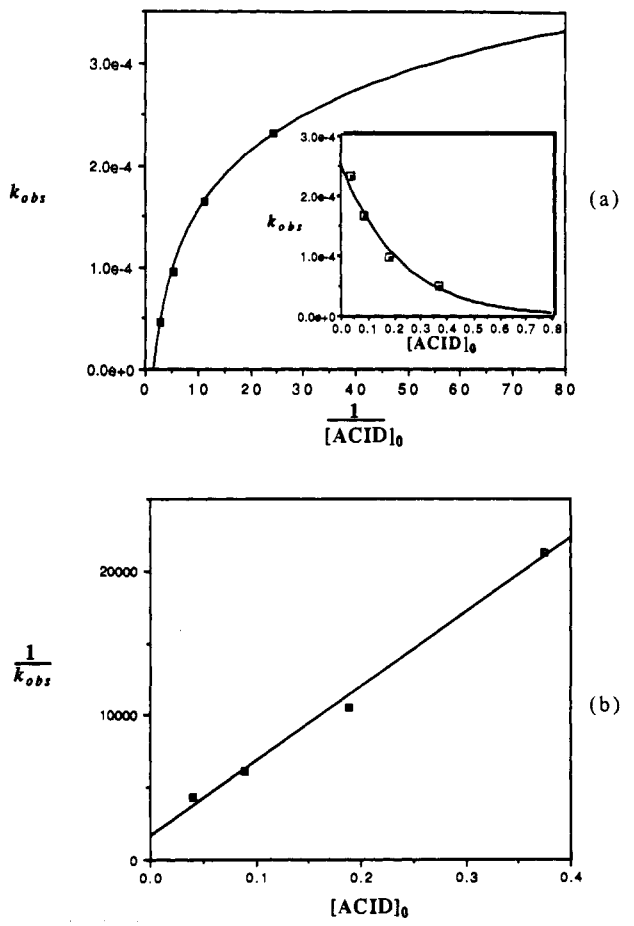

Figure 3. (a) Observed rate of decarboxyltion of cyanoacetic acid as a function of the inverse initial acid concentration. The inset graph depicts the observed rate of decarboxylation as a function of initial acid concentration showing the exponential decay in rate as the initial acid concentration is increased. (b) k_{obs}^{-1} as a function of initial acid concentration. The intercept indicates the maximum rate constant for the decarboxylation.

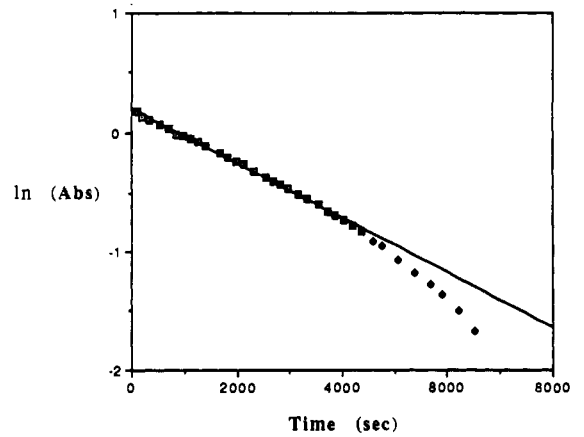

Figure 4. Typical pseudo-first-order rate plot for the disappearance of cyanoacetic acid in the presence of **2** at 72 °C. The initial data are essentially linear, but the rate begins to increase toward the end of the reaction when the acid is nearly consumed and the equilibrium between **2** and **3** shifts to afford significantly more of complex **2**.

decarboxylation increased by a factor of 2.1 relative to an identical run under 500 psi of nitrogen. This increase in rate is understood if we consider the fact that $W(CO)_5NCCH_2COOH$ (the *inactive* tungsten complex) has been shown to react with CO (independent of CO pressure above 200 psi) in THF with a rate constant of 1.27×10^{-3} s^{-1} at 65 °C with quantitative formation of $W(CO)_6$.[5] This process is fast relative to the decarboxylation process.

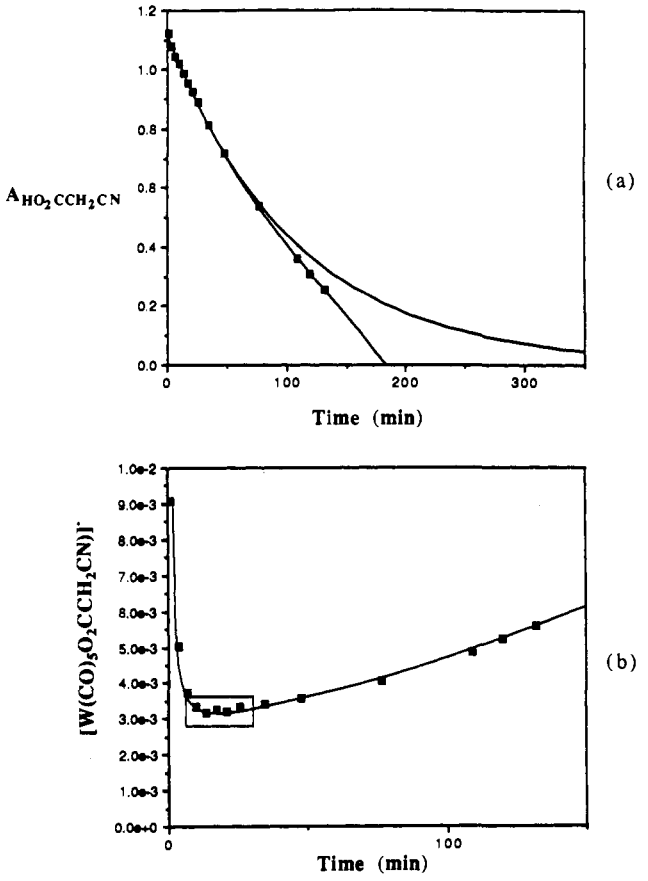

Figure 5. (a) Infrared absorbance of cyanoacetic acid as a function of time. Note the exponential rate of decay of acid which increases during the second half of the reaction due to the increase in [**2**]. (b) Concentration of **2** as a function of time during the decarboxylation reaction. The amount of **2** in solution decreases rapidly, remains constant (the boxed area, which corresponds to the exponential part of the curve in Figure 5a), and then slowly increases during the second half of the reaction.

Table I. Rate Constants as a Function of Temperature for the Catalytic Decarboxylation of Cyanoacetic Acid by $[PPN][W(CO)_5O_2CCH_2CN]^a$

temp (°C)	10^4k_{obs} (s^{-1})	10^2k_2 (M^{-1} s^{-1})^b
56.0	0.367	1.45
60.0	0.605	2.17
64.0	0.944	3.12
68.0	1.61	4.92
72.0	2.30	6.56

^{a} Reactions were carried out in DME solution. ^{b} The concentration of $W(CO)_5O_2CCH_2CN^-$ was obtained from a Beer's law plot after the initial equilibrium position in eq 4 was reached.

Subsequently, $W(CO)_6$ rapidly reacts with cyanoacetate to reform complex **2**. Hence, the net effect of added CO is to temporarily enhance the concentration of **2** and accelerate the rate of decarboxylation. This effect counterbalances the inhibitory effect of CO anticipated based on it occupying the active site at the metal center for substrate binding (vide infra). The process is, however, inhibited by acetonitrile. In the presence of 15.5 equiv of acetonitrile, the observed rate of decarboxylation was $k = 7.80 \times 10^{-5}$ s^{-1} at 65 °C (see Experimental Section). This is indeed slower than the case in which no acetonitrile is added at the beginning of the reaction, where the rate was calculated from Figure 3a to be $k = 1.08 \times 10^{-4}$ s^{-1}.

The facile decarboxylation of cyanoacetic acid by **2** does not appear to be applicable for other carboxylic acids. That is, we found no other carboxylic acids that were decarboxylated by **2**, even in instances in which the acid strength of the carboxylic acid was similar to that of HO_2CCH_2CN. In the case of $ClCH_2$-

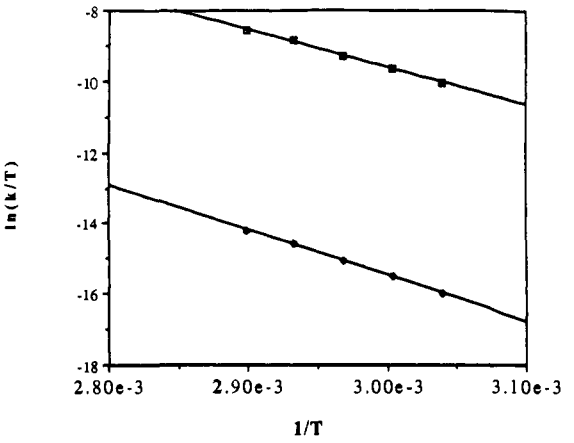

Figure 6. Eyring plot for the catalytic decarboxylation reaction: (□) = second-order rate constants, (◆) = pseudo-first-order rate constants.

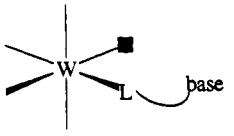

■ = vacant site

Figure 7. General form of complexes which act as catalysts for the decarboxylation of cyanoacetic acid.

COOH, of which the pK_a is 2.8 as compared with a value of 2.5 found for $CNCH_2COOH$, only one turnover resulted. Addition of $ClCH_2COOH$ to **2** resulted in formation of 1 equiv of CO_2 and CH_3CN. The chloroacetic acid, however, did not catalytically decarboxylate. After 1.5 h at 65 °C, no loss of $ClCH_2COOH$ had occurred; conversely, in the analogous reaction with $CNCH_2COOH$, 5.75 turnovers had occurred in 1.5 h. An important difference seems to be the fact that chloroacetic acid does not interact strongly with the metal in its protonated form. Whereas cyanoacetic acid formed a very stable complex (**3**) with tungsten, attempts at synthesizing the chloro-analog to **3**, $W(CO)_5ClCH_2COOH$, from $W(CO)_5THF$ and $ClCH_2COOH$ were unsuccessful.

On the other hand, tungsten(0) complexes possessing properties in common with those of complex **2** similarly exhibit catalytic activity for the decarboxylation of cyanoacetic acid. For example, complexes of the type illustrated in cartoon form in Figure 7, where the active site at tungsten is created by protonation of the chelated base, are also catalysts for this decarboxylation (eq 6).

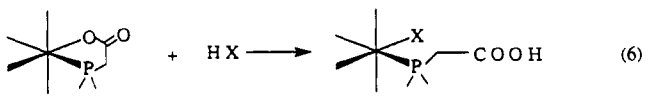

(6)

These differ from complex **2**, where the active site is a result of the CO-labilizing ability of the oxygen donor ligand. The relative catalytic activity, as indicated by their respective k_2 (M^{-1} s^{-1}) values at 65 °C, for the decarboxylation of cyanoacetic acid for various

ligands is $-O_2CCH_2CN^-$ (3.3×10^{-2}) ≫ $-PPh_2(CH_2)S^-$ (6.9×10^{-4}) > $-PPh_2CH_2CO_2^-$ (4.4×10^{-4}) ≫ $-PPh_2(CH_2)_2NMe_2$.

Discussion

The observations noted in our studies of the mechanistic aspects of the catalytic decarboxylation of cyanoacetic acid via the precursor complex $W(CO)_5O_2CCH_2CN^-$ are consistent with the

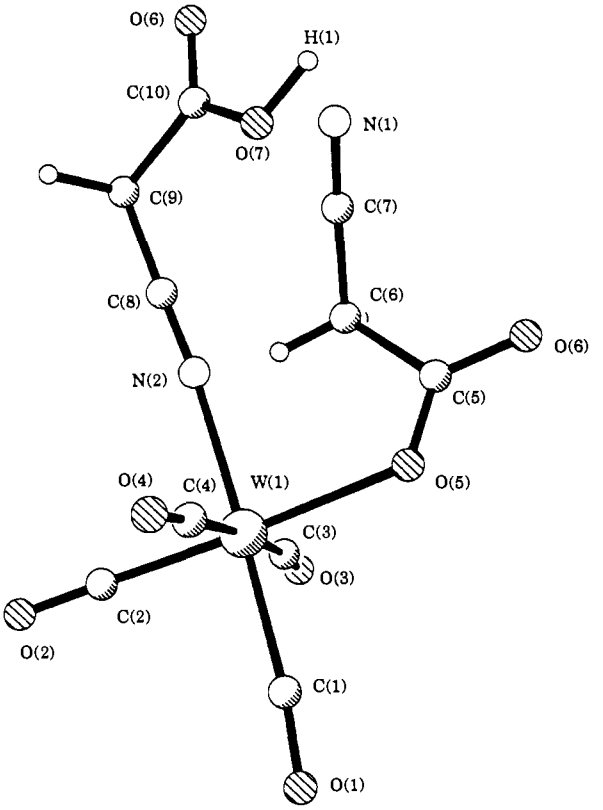

Figure 8. Molecular model of the proposed intermediate *cis*-$W(CO)_4O_2CCH_2CN(NCCH_2COOH)^-$ rotated to show the closest interaction between H(1) and N(1).

Scheme I

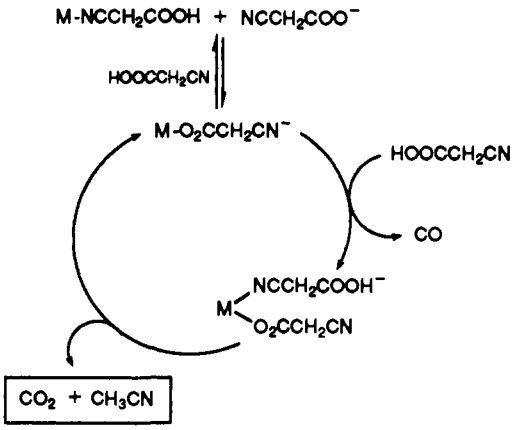

reaction cycle shown in Scheme I. The rate-limiting step is loss of CO from complex **2** with complexation of the substrate $NCCH_2COOH$ to afford the unstable intermediate *cis*-$W(CO)_4(O_2CCH_2CN)(NCCH_2COOH)^-$. The free energies of activation are nearly identical for the *decarboxylation* and *CO dissociation* processes at 22.0 ± 0.8 kcal·mol^{-1} and 23.0 ± 0.9 kcal·mol^{-1},[4] respectively. Further support for this interpretation came from the observation that upon elimination of the thermal barrier for CO dissociation via photolysis, decarboxylation occurs rapidly. It is noteworthy here to point out that because of the electron-withdrawing nature of the $-CH_2CN$ substituent, the cyanoacetate ligand has no propensity to form an oxygen-chelated species of the form $W(CO)_4(\eta^2\text{-}O_2CCH_2CN)^-$. Hence, there is no competition of the distal oxygen atom of the carboxylate with the substrate for binding at the metal center in this instance. In subsequent faster steps, decarboxylation occurs with formation of acetonitrile and carbon dioxide.

We can hypothesize about the more rapid steps that ensue

Scheme II

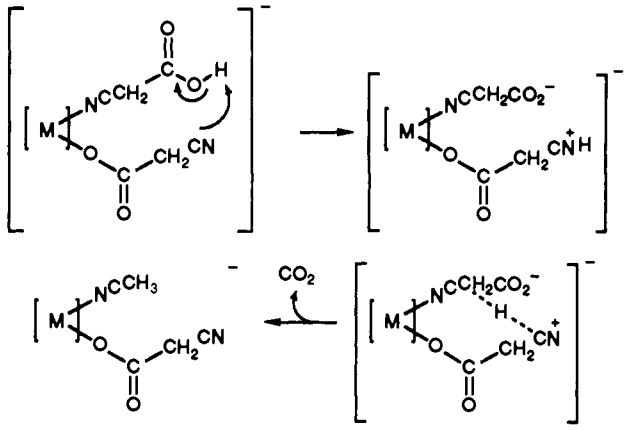

Scheme III

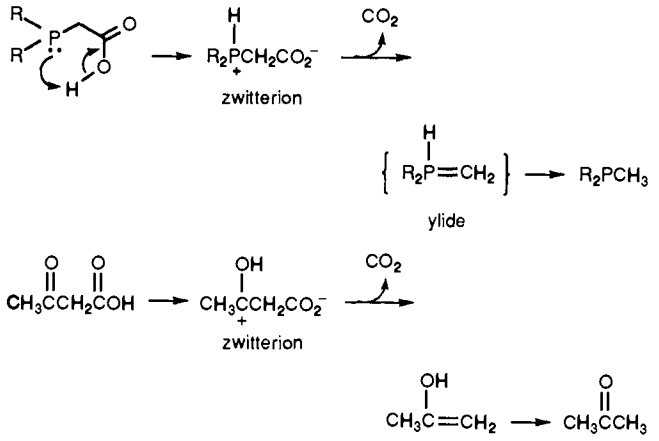

succeeding substrate–metal binding based on literature precedent and molecular modeling studies. That is, the next step involves intramolecular proton transfer between the N-bound acid and the carboxylate ligand via its nitrile function. This process is shown to be quite feasible from molecular modeling studies as is illustrated in Figure 8. It is noteworthy that in the solid-state structure of the β-form of free cyanoacetic acid,[9] the two independent molecules are linked together by an O–H···N hydrogen bonding motif. Decarboxylation occurs with the incipient anion being stabilized by metal binding followed by reprotonation to provide acetonitrile. Consistent with this interpretation, it was demonstrated (see Experimental Section) that the esterified analog of the proposed intermediate in the decarboxylation process, *cis*-$W(CO)_4(O_2CCH_2CN)(NCCH_2COOEt)^-$, was stable with respect to decarboxylation. As expected, one of the products of decarboxylation, CH_3CN, should inhibit the catalysis by binding to the metal center. This was indeed observed upon addition of acetonitrile to the reaction system. Hence, the roles ascribed to the metal are to provide a ligand with a basic site for intramolecular proton transfer and to stabilize the developing anion afforded upon loss of CO_2 (Scheme II). Similar intramolecular protonation processes have accounted for the mechanistic observations for the decarboxylation of acetylacetic and phosphinoacetic acids (~100 °C) (Scheme III).[10,11]

In an effort to further test this working hypothesis, we investigated the use of specifically designed metal complexes

Scheme IV

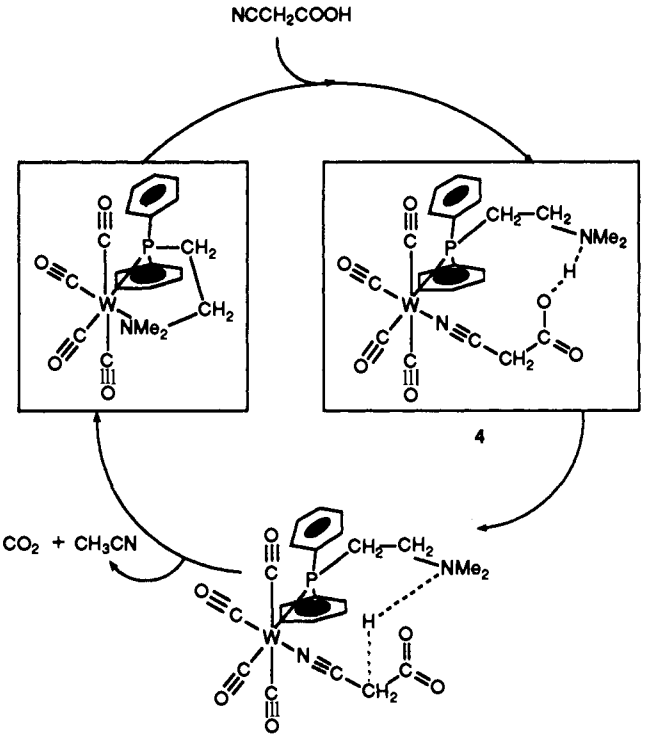

having the above characteristics, as catalysts for the decarboxylation of cyanoacetic acid. These studies included both anionic and neutral chelated complexes, i.e., $W(CO_4(PPh_2CH_2CO_2)^-$, $W(CO)_4(PPh_2CH_2CH_2S)^-$, and $W(CO)_4(PPh_2CH_2CH_2NMe_2)$. The three derivatives possess an appended ligand that is readily protonated by the acid substrate concomitantly providing a site for substrate binding at the metal center. Indeed, these derivatives exhibit catalytic activity for the decarboxylation of cyanoacetic acid with the relative reactivity of these vs complex **2** being $-O_2CCH_2CN^-$ (67) > $-PPh_2CH_2CH_2S^-$ (1.6) > $-PPh_2CH_2CO_2^-$ (1.0 > $-PPh_2CH_2CH_2NMe_2$ ($\ll$1.0). This order of reactivity inversely correlates with the base strength of the proton acceptor.

During the catalytic decarboxylation of cyanoacetic acid using $W(CO)_4(PPh_2CH_2CH_2NMe_2)$, where decarboxylation was slow, it was possible to spectroscopically identify the intermediate **4** in Scheme IV (see Figure 9). The proton in species **4** is indicated as being associated with both the carboxylate and $-NMe_2$ functions, since no infrared bands assignable to the free ν_{COO} functionality were observed. Because of the large excess of acid present in the catalytic system, it was not possible to directly observe hydrogen bonding in the proposed intermediate by infrared spectroscopy. However, experiments are underway to isolate species **4** and fully characterize it both in the solid state and in solution. After all of the $NCCH_2COOH$ is converted to acetonitrile and carbon dioxide, the infrared spectrum of the reaction mixture indicates that the parent complex, $W(CO)_4(PPh_2CH_2CH_2NMe_2)$, has quantitatively reformed. As anticipated for reactions involving these types of catalytic precursors, i.e., devoid of a CO-labilizing ligand, the decarboxylation process is quenched in the presence of high carbon monoxide concentrations that effectively block the binding site for the acid substrate.

Concluding Remarks

Despite the fact that in general, aliphatic carboxylic acids (RCOOH) undergo decarboxylation at temperatures greater than 300 °C,[12] strongly electron-attracting substituents (R) such as CCl_3, CN, or >C=O can greatly facilitate this process. This is

(9) (a) Kanters, G. R.; Straver, L. H. *Acta Crystallogr., Sect. B: Struct. Sci.* **1978**, *B34*, 1393. (b) Kanters, G. R.; Roelofsen, G.; Straver, L. H. *Acta Crystallogr., Sect. B: Struct. Sci.* **1978**, *B34*, 1396.

(10) Widmark, J. *Acta Med. Scand.* **1920**, *53*, 393; *Chem. Abstr.* **1921**, *15*, 2763.

(11) (a) Mann, F. G.; Tong, B. P.; Wystrack, V. P. *J. Chem. Soc.* **1963**, 1155. (b) Ludvik, J.; Podlahova, J. *J. Inorg. Nucl. Chem.* **1978**, *40*, 967. (c) van Doorn, J. A.; Meijboom, N. *J. Chem. Soc., Perkin Trans. II* **1989**, 1309.

(12) Deacon, G. B.; Faulks, S. J.; Pain, G. N. *Adv. Organomet. Chem.* **1986**, *25*, 237.

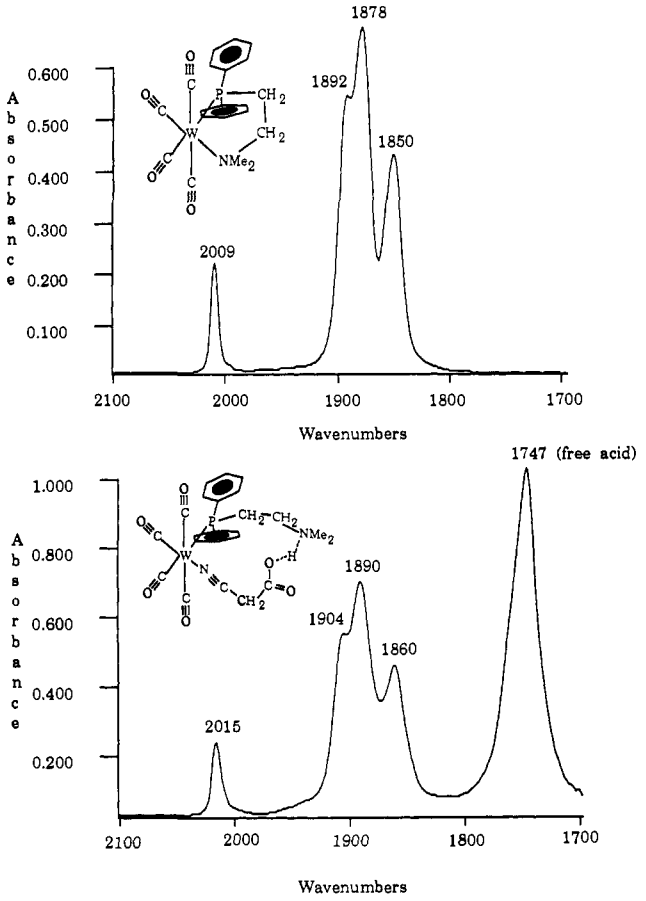

Figure 9. Infrared spectra of $W(CO)_4(\eta^2\text{-}PPh_2CH_2CH_2NMe_2)$ and intermediate **4** (ν_{CO} region) in DME solution. The ν_{CO} spectrum of the intermediate is shifted approximately 10 cm^{-1} to higher energy, as expected for a nitrile ligand replacing an amine ligand.

understandable in terms of a pathway involving heterolytic bond cleavage where the R group departs with an electron pair, i.e., $RCO_2^- \rightarrow R^- + CO_2$. Furthermore, these activated acids possess weakened C–CO_2^- bonds. As indicated in Scheme III, Ph_2PCH_2-COOH undergoes decarboxylation under rather mild conditions (100 °C) by way of intramolecular proton transfer to afford the zwitterion. An analogous process involving cyanoacetic acid would require the disruption of the very stable C≡N: bond (species **5**). Hence this uncatalyzed process has a much higher

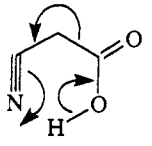

5

energy barrier, with decarboxylation occurring at 160 °C.[13] Conversely, binding of the phosphorus ligand of diphenylphosphinoacetic acid to the metal center has the expected result of greatly retarding the decarboxylation reaction of this acid.

Albeit complex **2** is an effective catalyst for decarboxylating cyanoacetic acid, especially when the substrate is pulsed into the reaction mixture, it is inferior to our recently reported Cu(I) catalysts for this process,[14] that is, Cu(I) catalysts not only are able to decarboxylate cyanoacetic acid at a much faster rate but are also effective catalysts for less activated carboxylic acids, e.g., 9-fluorenecarboxylic and malonic acids.[15] However, the metal carbonyl center of complex **2** and related derivatives allows for a detailed probe of the reaction pathway. It is concluded from these studies that the metal center in these instances provides a site for intramolecular proton transfer as well as serves to enhance the electron-withdrawing ability of the nitrile group resulting in a further weakening of the C–CO_2^- bond. Indeed the carbon–carbon bond distance in tungsten-bound $NCCH_2COOH$ is slightly longer than that observed in the free acid (1.512(9) Å vs 1.497(4) Å.[5]

A continuing goal of our research in this area is to affect the reverse process of decarboxylation, that is, the carboxylation of hydrocarbons to afford carboxylic acids from carbon dioxide. This process has only been accomplished to date for cases in which there is a good electron-withdrawing group (such as C≡N) on the α-carbon atom. For example, there are reports of the activation of *acidic* C–H bonds by electron-rich complexes of iridium(I) and rhodium(I) in the presence of carbon dioxide to provide the corresponding protonated metal cationic complex and carboxylate anion.[16-19] Nevertheless, these processes are not catalytic and are mechanistically not well defined.

Acknowledgment. The support of this research by the National Science Foundation (Grant CHE 91-19737) and the Robert A. Welch Foundation is gratefully acknowledged. We wish to thank Dr. Joseph Jászberényi for assistance with the GC/MS analyses. In addition, we are most thankful to Professor G. R. Dobson for a sample of $W(CO)_4(PPh_2CH_2CH_2NMe_2)$.

Supplementary Material Available: Pseudo-first-order rate plots for the decarboxylation of cyanoacetic acid catalyzed by $W(CO)_4(PPh_2CH_2CO_2)^-$ and $W(CO)_4(PPh_2CH_2CH_2S)^-$ (3 pages). Ordering information is given on any current masthead page.

(13) *Dictionary of Organic Compounds*; Heilbron, H., Ed.; Oxford University Press: New York, 1943; p 586.
(14) Darensbourg, D. J.; Longridge, E. M.; Atnip, E. V.; Reibenspies, J. H. *Inorg. Chem.* **1992**, *31*, 3951.
(15) (a) Toussaint, O.; Capdevielle, P.; Maumy, M. *Synthesis* **1986**, 1029. (b) Toussaint, O.; Capdevielle, P.; Maumy, M. *Tetrahedron* **1984**, *40*, 3229. (c) Toussaint, O.; Capdevielle, P.; Maumy, M. *Tetrahedron Lett.* **1987**, *28*, 539.
(16) Behr, A.; Herdtweck, E.; Herrmann, W. A.; Keim, W.; Kipshagen, W. *Organometallics* **1987**, *6*, 2307.
(17) Behr, A. *Carbon Dioxide Activation by Metal Complexes*; VCH Publishing: Weinheim, West Germany, 1988.
(18) English, A. D.; Herskovitz, T. *J. Am. Chem. Soc.* **1977**, *99*, 1648.
(19) Ittel, S. D.; Tolman, C. A.; English, A. D.; Jesson, J. P. *J. Am. Chem. Soc.* **1978**, *100*, 7577.